



DEVELOPMENT OF FRAGILITY CURVES FOR LARGE-SCALE SEISMIC RISK OF RC STRUCTURES

R. Monteiro⁽¹⁾, A. Abarca⁽²⁾, G. O'Reilly⁽³⁾, S. Kechidi⁽⁴⁾, D. Bellotti⁽⁵⁾, B. Borzi⁽⁶⁾, J.M. Castro⁽⁷⁾

⁽¹⁾ Associate Professor, University School of Advanced Study IUSS Pavia, ricardo.monteiro@iusspavia.it

⁽²⁾ PhD Candidate, University School of Advanced Study IUSS Pavia, andres.abarca@iusspavia.it

⁽³⁾ Assistant Professor, University School of Advanced Study IUSS Pavia, gerard.oreilly@iusspavia.it

⁽⁴⁾ Researcher, University of Porto Faculty of Engineering (FEUP), kechidi@fe.up.pt

⁽⁵⁾ Researcher, European Centre for Training and Research in Earthquake Engineering, davide.bellotti@eucentre.it

⁽⁶⁾ Senior Researcher, European Centre for Training and Research in Earthquake Engineering, barbara.borzi@eucentre.it

⁽⁷⁾ Assistant Professor, University of Porto Faculty of Engineering (FEUP), miguel.castro@fe.up.pt

Abstract

Large-scale earthquake risk assessment has proven to be a valuable tool to provide guidance in the definition and implementation of disaster risk reduction measures. Such an assessment often requires simplified analyses to process the great amount of data that is needed to characterize the problem of earthquake risk in each of its three main components: hazard, exposure and vulnerability. The use of fragility functions represents a convenient tool to estimate the probabilistic damage distribution of a set of structures as a function of simple ground motion parameters. To obtain such fragility functions from a large-scale perspective, a comprehensive set of assumptions can be made to estimate the response of multiple different structures within the same construction typology, when subjected to a set of ground motions with increasing intensities. The observed behavior of each system is then linked to a level of damage and the overall results can be processed statistically and correlated with the applied ground motion characteristics to determine an adequate continuous function that can relate a damage distribution to a seismic intensity measure. This paper focuses specifically on the vulnerability models developed in the context of two recent EU-funded projects for large-scale assessment of structures: ITERATE (Improved Tools for Disaster Risk Mitigation in Algeria, www.iterate-eu.org) that dealt with the residential building stock in Blida, Northern Algeria; and INFRA-NAT (Increased Resilience of Critical Infrastructure to Natural and Human-Induced Hazards, www.infra-nat.eu) that dealt with the reinforced concrete bridge inventory of Italy, North Macedonia and Israel. In particular, the paper describes the assumptions and the adopted analysis procedures to determine fragility functions for the main structural typologies that were identified in both cases, underlining the different challenges and opportunities for each methodology, as well as the resulting fragility functions that were developed for each case.

Keywords: *buildings, bridges, seismic risk, fragility curves, regional scale.*



1. Introduction

The structural and non-structural damage observed during past earthquakes [1-3] demonstrated the need for simplified tools to perform seismic risk assessment and to evaluate economic losses both at single and regional scale [4-6]. The latter has proven to be a valuable tool to provide guidance in the definition and implementation of Disaster Risk Reduction (DRR) measures. Such assessment often requires a simplified analysis to process the great amount of information that is needed to characterize the problem of earthquake risk in each of its three main components: hazard, exposure and vulnerability.

In terms of vulnerability, the use of fragility functions represents a convenient tool to estimate the probabilistic damage distribution of a set of structures as a function of simple ground motion parameters. To obtain such fragility functions, a comprehensive set of assumptions can be made to estimate the response of multiple different structures within the same construction typology, when subjected to a set of ground motions which are scaled to increasing intensity levels. Furthermore, the results of damage can be processed statistically and correlated with the applied ground motion characteristics to determine an adequate continuous function that can associate a damage distribution with an earthquake intensity measure.

This study deals with the description of the assumptions that were made and the analysis procedure that was adopted to develop fragility models in the context of two recent EU-funded projects for large-scale assessment of structures: ITERATE (Improved Tools for Disaster Risk Mitigation in Algeria, www.iterate-eu.org) that dealt with the residential building stock in Blida, Northern Algeria; and INFRANAT (Increased Resilience of Critical Infrastructure to Natural and Human-Induced Hazards, www.infra-nat.eu) that dealt with the reinforced concrete bridge inventory of Italy, North Macedonia and Israel.

In both projects, a taxonomy-based approach was used, however, based on the inherent limitations and opportunities in each case, the analysis methodology to derive the fragility curves was different. The specific differences between the methods will be discussed herein, as well as the strengths and deficiencies found in each case.

2. Methodology

Two methodologies were adopted for the calculation of fragility curves based on the specific characteristics of each project.

In the case of the ITERATE Project, given that the scope of calculating fragility curves for the entire building stock of Algeria was very ambitious, involving a wide variety of structural types with very different systems and characteristics that lead to a wide range in structural behavior, a more simplified approach needed to be selected to be able to manage the analysis workload and computational requirements within the available timeframe and resources. Therefore, the methodology defined for creating fragility curves for each taxonomy branch in ITERATE followed the procedure used by Villar-Vega [7] in which multiple references were consulted to obtain a wide set of capacity curves for each of the building typologies identified as part of the Algerian residential building inventory. The structural behavior of each typology was represented by the average capacity curve obtained from this previous step, which was then used to create a large number of synthetic equivalent single-degree-of-freedom (SDOF) oscillators that represent the building-to-building variability of the entire inventory.

Afterwards, a large set of ground motion records of increasing intensity was defined to represent the record-to-record variability and both of these components of variability were combined through a series of nonlinear time history analyses, leading to a distribution of damage per ground motion intensity level. A schematic representation of this process is shown in Fig. 1.

In the case of the INFRA-NAT project, given that the scope focused only on bridge inventories, which are more uniform in terms of structural typologies, as well as being structurally more straightforward to assess (when regular) than buildings, a more detailed analysis process was permitted for the derivation of their fragility curves.

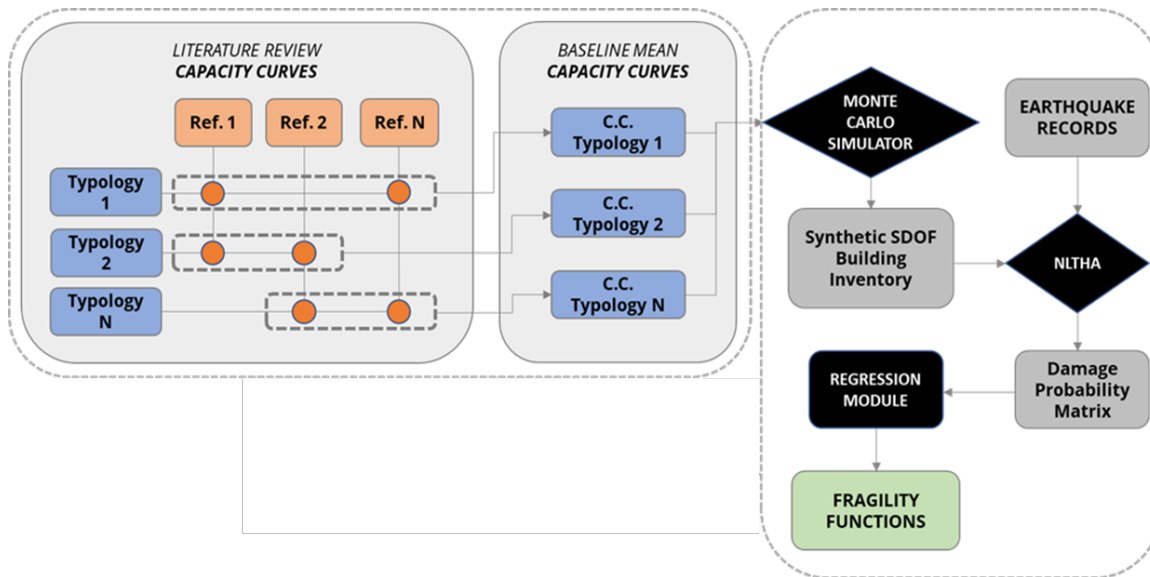


Fig. 1 – Schematic representation of the methodology implemented for the ITERATE Project

In that case, thus, a numerical modelling framework was implemented to produce sets of synthetic numerical models that were collectively characteristic of the taxonomy groups they represented and each taxonomy branch was studied in detail to determine the variations of characteristic properties in each set that would influence the most the structural behaviour of the group.

An analysis platform was then used to perform nonlinear time-history analysis (NLTHA) of each synthetic bridge model with a set of ground motion records of increasing intensity measure level that were previously defined in the INFRA-NAT project for each participating country [8]. The resulting performance of each bridge-accelerogram pair was assessed using a damage criterion to determine the probability of exceeding a specific limit state, leading to a damage probability matrix. The observed values in the matrix were then evaluated in a regression module to determine the best fitting continuous function that describes the probability of exceedance of each limit state for any individual synthetic bridge model as a function of ground motion shaking intensity level. Finally, all resulting fragility curves belonging to a same taxonomy branch were statistically combined in order to derive a single fragility curve representative of the real bridges in the group. A schematic representation of this process is shown in Fig. 2.

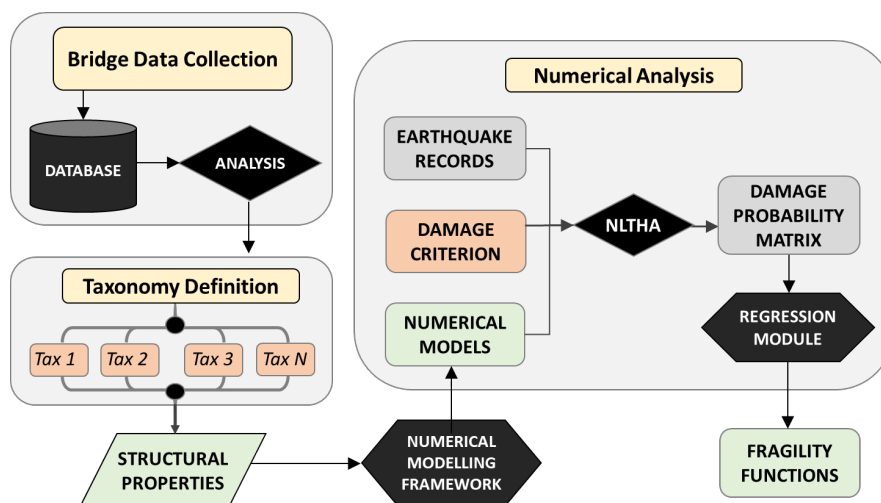


Fig. 2 – Schematic representation of the methodology implemented for the INFRA-NAT Project



3. Taxonomy definition

Given the large amount of assets that are part of the inventories of large-scale assessment projects, structures are evaluated not individually using their specific information, but rather grouped and categorized according to taxonomy schemes. These schemes are defined on the basis of key structural properties available for a large number of the assets in the inventories, under the assumption that, on average, structures classified under the same taxonomy have similar performance under similar seismic intensities. The definition of the structural characteristics that define the choice of the taxonomies were determined for both projects based on expert opinion and common practice, as well as being limited to the available information in the assembled databases. The building parameters and resulting taxonomy branches evaluated for the ITERATE project are shown in Table 1, while the full bridge taxonomy defined for the INFRA-NAT project is presented in Table 2.

Table 1 – Taxonomy definition for the building stock analyzed in the ITERATE project

Construction type	Number of floors	Design level	Taxonomy code
RC moment resisting frames	Low-rise (1-3)	Medium-code	RC MRF LR MC
		Post-code	RC MRF LR PC
	Mid-rise (4-7)	Pre-code	RC MRF MR PC
RC shear wall	Mid-rise (4-7)	Post-code	RC SW MR PC
	high-rise (>7)	Post-code	RC SW HR PC
Dual RC: moment resisting frames and shear walls	Low-rise (1-3)	Post-code	RC MRF-SW LR PC
		Pre-code	RC MRF-SW MR PC
	Mid-rise (4-7)	Medium-code	RC MRF-SW MR MC
		Post-code	RC MRF-SW MR PC
	High-rise (>7)	Pre-code	RC MRF-SW HR PC
		Medium-code	RC MRF-SW HR MC
Unreinforced Masonry	Low-rise (1-3)	Pre-code	UM LR PC

Table 2 – Taxonomy definition for the building stock analyzed in the ITERATE project

Country	Material	Spans	Static Scheme	Deck Type	Pier Type	Taxonomy Code
Italy	Reinforced Concrete	2 to 4	Simply Supported	Beam	Multiple Column	RC-2/4-SS-B-MC
					Wall	RC-2/4-SS-B-W
			Frame	Plate	Any	RC-2/4-F-P
Above 5		Simply Supported	Beam	Multiple Column	RC-5+-SS-B-MC	
				Wall	RC-5+-SS-B-W	
				Single Column	RC-5+-SS-B-SC	
North Macedonia		2	Simply Supported	Beam	Wall	RC-2-SS-B-W
						RC-3-SS-B-W
						RC-4-SS-B-W
						RC-3-F-P-W
Israel		2 or 3	Continuous	Beam	Multiple Column	RC-2/3-C-B-MC
						RC-2/3-F-B-MC
	RC-2/3-F-B-W					
	4 or 5	Simply Supported	Beam	Multiple Column	RC-4/5-SS-B-MC	
					RC-4/5-C-B-MC	
		Continuous	Box	Wall	RC-4/5-C-BO-W	
				Single Column	RC-4/5-C-BO-SC	
		Frame	Beam	Multiple Column	RC-4/5-F-B-MC	
			Plate	Single Column	RC-4/5-F-P-SC	
Above 6	Simply Supported	Beam	Single Column	RC-6+-SS-B-SC		
			Multiple Column	RC-6+-SS-B-MC		



4. Numerical Modelling

Within the ITERATE project, building-to-building variability was accounted for by generating a set of synthetic SDOF models, obtained through Monte Carlo simulation, which considered the baseline capacity curves taken from literature as the mean curve, and generated 200 normally distributed curves. To determine the statistical parameters to be used in the simulation, 3D structural models of buildings that matched the most representative typologies of the inventory were analyzed through nonlinear static analysis using a first-mode proportional lateral loading pattern to obtain capacity (*pushover*) curves of each structure.

These parameters were then used to run a Monte Carlo simulation using the GEM Foundation's Risk Modeller Toolkit [9] to generate 200 compatible synthetic capacity curves. As in previous studies [7], the variability was assumed as uncorrelated and following a normal distribution. The results for the aforementioned building typology are shown in Fig. 3, where the modelled curves are compared side by side with the generated inventory. Given the lack of blueprints for more typologies, the statistical coefficient of variation parameters of the modelled building class was used for the remaining typologies, taking, for each, the mean capacity curve that was obtained from the literature review [10].

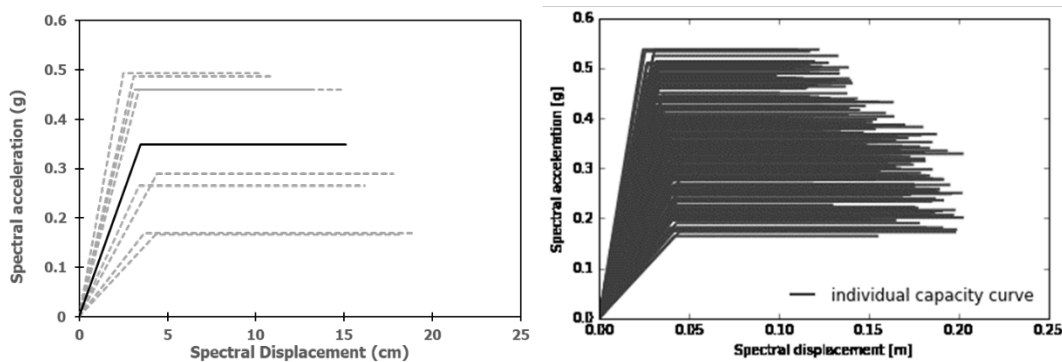


Fig. 3 – Comparison of capacity curves from structural models (left) and 200 generated compatible capacity curves (right), for the RC-MRF-LR-C typology of the ITERATE project

In the case of INFRA-NAT, a state-of-the-art tool developed by the Eucentre Foundation, called B.R.I.T.N.E.Y (BRidge auTomatic Nonlinear analysis based Earthquake fragilitY) [11], was used. The tool creates finite element models for carrying out nonlinear time-history (NLTH) analysis within the OpenSees environment [12] and processes the results to obtain fragility functions for each bridge. An example of the models created by the tool for a bridge is shown in Fig. 4.

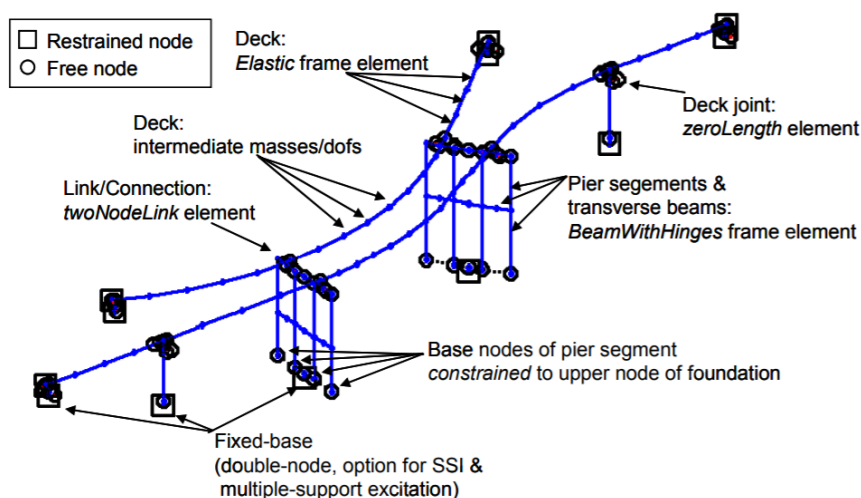


Fig. 4 – Example of numerical model of a bridge created using BRITNEY [10]



Given that very few assets in the inventory had enough information to produce specific numerical models, the BRITNEY tool was used to generate synthetic sets of bridges for each taxonomy branch with samples from the distribution of structural characteristics found in the inventory. Conceptually, this is a similar approach to the one based on random sampling that was employed for the residential building stock however this time referring to the different parameters of full 3D models, rather than equivalent SODF systems.

In order to define the number of synthetic models required to capture the entire range of behavior for a given taxonomy branch, a sensitivity analysis was carried out where multiple bridge model idealizations were created and the evolution of the mean fragility results was tracked until the mean and standard deviation values for all limit states defined became stable under a reasonable tolerance level (variations of under 5%). An example of such analysis is shown in Fig. 5.

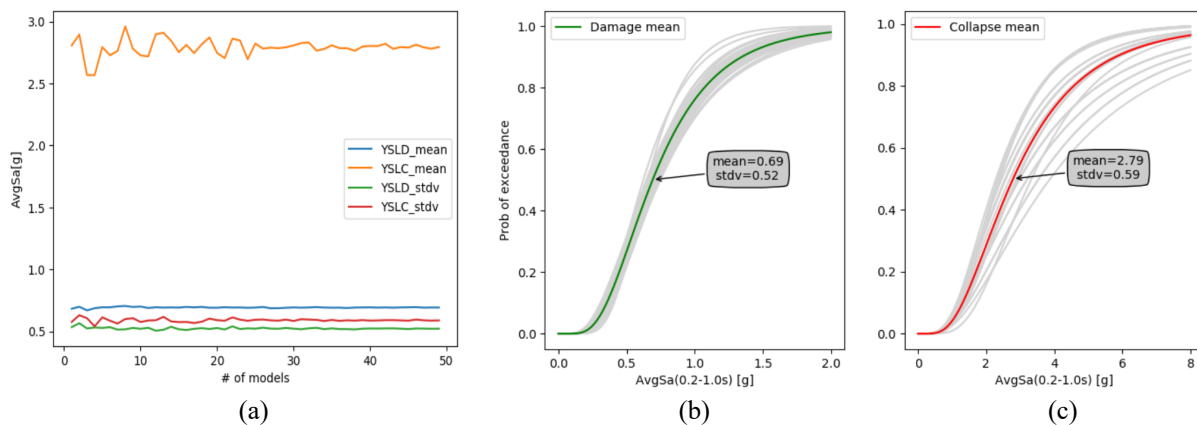


Fig. 4 – Example of (a) evolution of mean results based on number of synthetic models, and resulting (b) Damage and (c) Collapse fragility curves for the INFRA-NAT RC-4-SS-B-W taxonomy branch

In all cases, it was found that a number between 30 and 50 bridge models, sampled from the structural characteristic parameters, led to stable results for each taxonomy branch; the actual number depended on the homogeneity level of properties in the assets of each taxonomy branch.

5. Selection of Earthquake Records

Both projects made use of sets of earthquake records in order to perform the NLTH analysis required for the determination of the fragility curves, however, the selection method used to define the records was substantially different between both. For the ITERATE case, the selection was made on the basis of compatibility with the uniform hazard spectra (UHS) of the city of Blida for a return period of 475 years, from records publicly available in the PEER (Pacific Earthquake Engineering Research) database using the Harmony Search algorithm implemented in the SeIEQ tool [13], imposing that the average spectrum of the complete set would not deviate from the target by more than 10% at any point. The response spectra for the 40 selected records are shown in Fig. 5. The same selected records were then scaled to represent at least 10 levels of return period, ranging from 50 years to 50,000 years.

On the other hand, for the INFRA-NAT case, the selection was made following a recasting of conditional spectrum record selection based on AvgSa [14], for a period range of $T_{lower}=0.20s$ and $T_{upper}=1.0s$, which was chosen to encompass the entire period range of the bridge inventories. A composite database, comprising the PEER NGA-West2 database (<https://ngawest2.berkeley.edu/>) and the Engineering-Strong Motion (ESM) database (<https://esm.mi.ingv.it/>) was used to select the accelerograms. Different sets of records were selected for six locations in Italy, six locations in North Macedonia, and four locations in Israel; each for seven considered return periods of ground shaking (98, 224, 475, 975, 2475, 4975 and 9975 years) for a total of 42 sets for both Italy and North Macedonia and 28 for Israel. An example of a record set, together with the target spectrum, is shown in Fig. 6.

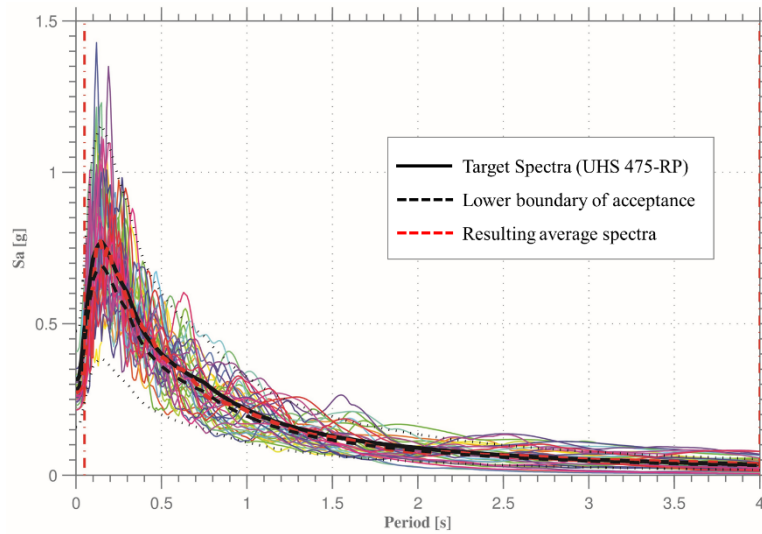


Fig. 5 – Response spectra for selected records scaled to match 475-year R.P. UHS for Blida, Algeria

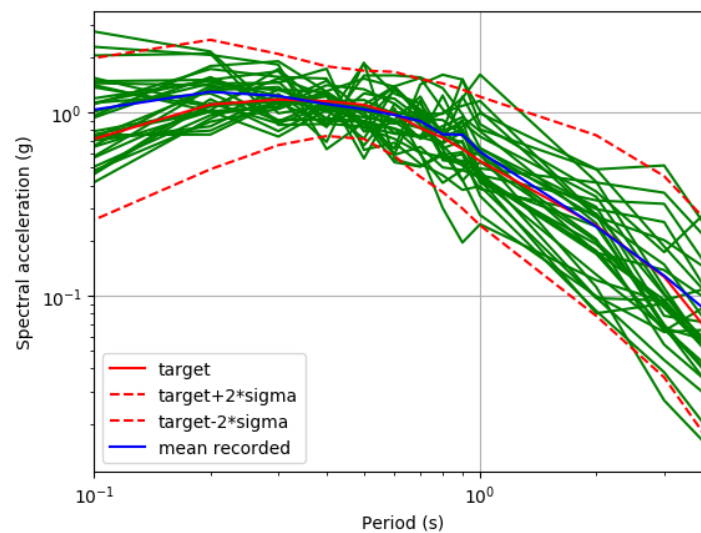


Fig. 6 – Conditional spectrum AvgSa-based record selection performed for site 4 in Italy, considering the 2475-year return period

6. Definition of Limit States and Damage Criterion

For the ITERATE project, given that the structures were represented numerically as very simple SDOF models that only account only for spectral displacement and base shear, the limit states were defined only in terms of relative displacement between the yield and ultimate points, i.e., ductility capacity of each model.

Within this context, four damage states were considered: slight, moderate, extensive and collapse. The slight damage state was defined as corresponding to the attainment of 60% of the yield displacement (i.e., $0.6 S_{d_y}$) and the moderate damage when the yielding displacement is exceeded (i.e., S_{d_y}). The threshold for extensive damage was defined as the mean between the yielding and the ultimate spectral displacement (i.e., $(S_{d_y} + S_{d_u})/2$), and collapse when the displacement of the system exceeds the 80% of the ductility capacity (i.e., $S_{d_y} + 0.8(S_{d_u} - S_{d_y})$) as illustrated graphically in Fig. 7.

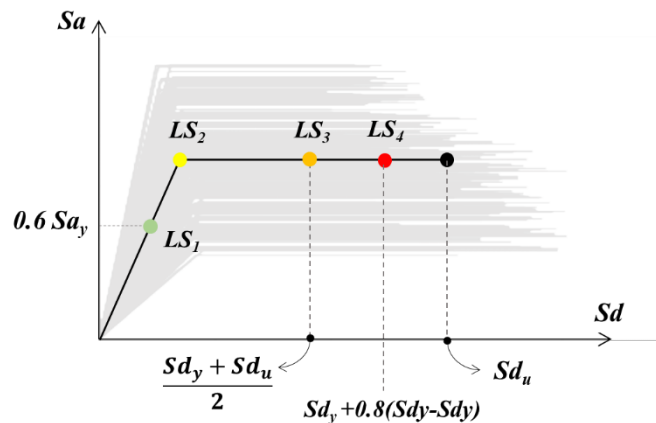


Fig. 7 – Graphic representation of the defined limit states on a capacity curve used for the ITERATE project. Slight (LS1), Moderate (LS2), Extensive (LS3) and Collapse (LS4)

For the case of the INFRA-NAT project, in order to be consistent with the BRITNEY analysis tool [11], two limit states were used for the classification of performance of the assets: a) damage limit state and b) collapse limit state. In this tool, structural deterioration interactions between elements leading to collapse was not specifically accounted for in the models (i.e. elements will deform beyond the limit response thresholds), but local bi-directional demand over capacity ratios were calculated for piers and bearings and, depending on the values of these ratios, damage states were later assigned in post-processing.

Unseating failure was checked at the bearing level: bearings could fail due to excessive displacement demand, from simple falling off the deck from the bearing seat or to the full loss of support from the pier head. The first condition detected relevant damage, while the second collapse. Displacement capacity of bearings is derived from the pier cap and bearing seats geometry, or directly defined by the user.

Two response thresholds were considered for pier chord rotation (yield θ_y and ultimate θ_u). Yield and ultimate curvatures were determined automatically from a bilinear fit of a section moment-curvature analysis to deal with general cross-section shapes and reinforcement layouts. In terms of shear failure, given the brittle nature of the phenomenon, only a single threshold was defined and associated with the collapsed limit state. The equations used in the definition of the pier thresholds for chord rotation and shear are presented in Table 3.

Table 3 – Capacity thresholds for pier segments adapted from [11]

Limit State	Mechanism	Equation
Damage	Flexure	$\theta_y = \frac{\phi_y L_p}{3}$
Collapse	Flexure	$\theta_u = \theta_y + (\phi_u - \phi_y) L_p \left(1 - \frac{L_p}{2L_v}\right)$ with: $L_p = 0.1L_v + 0.17h + 0.24 \left(\frac{d_b f_y}{\sqrt{f_c}}\right)$
	Shear	$V_u = V_c + V_N + V_s$ with: $V_c = k(\mu_\Delta) 0.8 A_c \sqrt{f_c}$ $V_s = A_{st} 0.9 h f_y$ $V_N = N \frac{0.8h}{2L_v}$

θ_y : yield chord rotation

θ_u : ultimate chord rotation

ϕ_y : yield curvature

ϕ_u : ultimate curvature

L_p : plastic hinge length

L_v : shear span length

$k(\mu_\Delta)$: ductility reduction coefficient

f_y : yield strength of steel

f_c : concrete compressive strength

A_{st} : shear steel area

A_c : confined concrete area

N : axial load



7. Development of Fragility Curves

For the ITERATE project, the derivation of the fragility functions for each building class was performed through NLTH analysis of SDOF systems using the GEM Foundation's Risk Modeller's Toolkit [9]. The analysis was performed on each of the 200 SDOF models, using the set of 40 selected ground motions, which were scaled to 10 different levels of intensity, leading to a total of 80,000 analysis per each taxonomy branch. For each, the maximum spectral displacement was computed and compared with the corresponding damage state thresholds shown previously in order to allocate the structure within a damage state. With this information, a damage probability matrix (DPM) was built for each building class, defining the fraction of buildings in each damage state, per ground motion record.

Once each damage state probability was calculated for each ground motion record, a cumulative probability curve was fitted to create the fragility functions for each typology through the logarithmic mean (λ) and standard deviation (β) that define a lognormal distribution, as described by Equation 1.

$$P[d_s|IM] = \Phi\left(\frac{\ln\left(\frac{IM}{\lambda}\right)}{\beta}\right) \quad \text{Eq. (1)}$$

For this purpose, the lognormal statistical parameters were calculated using the least squares regression method, first determining which spectral acceleration period provided the pair of logarithmic mean (λ) and logarithmic standard deviation (β) leading to the best correlation with the observed damage distribution. The GEM Foundation's Risk Modeller's Toolkit [9] performs this regression analysis by testing spectral acceleration at a wide range of structural periods and determines the average best fit for all damage states.

For the INFRA-NAT project, once the synthetic bridge models were defined and modelled, each asset was evaluated using NLTH analysis to each set of 30 bi-directional records, which formed a part of one of seven increasing intensity measure levels. Each individual record provided a small sample of response corresponding to demand values D in each vulnerable component to be compared to its corresponding component capacity values C , sampled from their respective distributions.

At each intensity level, the obtained sample of the component demand to capacity ratios $y=D/C$ was used to obtain a global, structural system level D/C ratio denoted by Y . Making the assumption that bridge components are a part of a series system, where the weakest failure system leads to the overall damage or collapse of the global structure, the global D/C ratio for the j -th intensity level and k -th ground motion is given in terms of the n local D/C ratios by Equation 2.

$$Y_{jk} = \max(y_{1jk}, \dots, y_{njk}) \quad j = 1, \dots, 7; \quad k = 1, \dots, 30 \quad \text{Eq. (1)}$$

The 30 values of Y at each intensity level were used to fit a lognormal distribution to determine the probability of exceedance of the unit value of Y that marked the exceedance of the performance level (limit state) being evaluated. These values of probability of exceedance form a piece wise fragility function. However, since a continuous function is desired for reference and ease of implementation in the platform, the points were assumed to follow a cumulative lognormal distribution and a maximum likelihood estimation (MLE) fitting algorithm [15] is employed to obtain the logarithmic mean (λ) and standard deviation (β) that define a lognormal distribution, as described by Equation 1.

The process was repeated for each synthetic bridge model in a specific taxonomy branch and the results were processed statistically to obtain a class fragility function that describes the fragility of the entire set of real assets in the portfolios assigned to that taxonomy branch.



8. Results

For the ITERATE project, the results of the logarithmic mean (λ) and standard deviation (β) that define the lognormal distribution of fragility curves are reported in Table 4 using as intensity measure the spectral acceleration at the structural period of best fit found for each taxonomy during the analysis process.

Table 4– Summary of fragility curves per typology using spectral acceleration at the structural period of best fit as IM for the taxonomies analyzed for the ITERATE project

Taxonomy	IM	Limit States							
		Slight		Moderate		Extensive		Collapse	
		λ	β	λ	β	λ	β	λ	β
RC MRF LR MC&C	Sa 1.0s (g)	0.143	0.033	0.229	0.069	0.660	0.185	0.871	0.202
RC MRF MR PC	Sa 1.0s (g)	0.105	0.026	0.159	0.040	0.260	0.074	0.325	0.100
RC MRF-SW LR PC	Sa 1.0s (g)	0.278	0.096	0.404	0.146	1.106	0.490	2.001	0.347
RC MRF-SW MR PC	Sa 0.7s (g)	0.133	0.036	0.200	0.047	0.431	0.145	0.556	0.205
RC MRF-SW MR MC	Sa 0.7s (g)	0.133	0.036	0.200	0.047	0.431	0.145	0.556	0.205
RC MRF-SW MR PC	Sa 1.0s (g)	0.347	0.094	0.532	0.167	1.120	0.350	2.153	0.590
RC MRF-SW HR PC	Sa 1.3s (g)	0.101	0.028	0.157	0.043	0.271	0.091	0.347	0.134
RC MRF-SW HR MC	Sa 1.3s (g)	0.101	0.028	0.157	0.043	0.271	0.091	0.347	0.134
RC MRF-SW HR PC	Sa 1.5s (g)	0.333	0.088	0.551	0.167	0.924	0.309	2.073	0.839

For the INFRA-NAT project, the results of the logarithmic mean (λ) and standard deviation (β) that define the lognormal distribution of fragility curves are reported in Table 5 using as intensity measure the average spectral acceleration AvgSa [14], for a period range of $T_{lower}=0.20s$ and $T_{upper}=1.0s$, in order to be consistent with the decision made during the record selection process.

Table 5 – Summary of fragility curves for the taxonomies analyzed for the INFRA-NAT project

Country	Taxonomy	Limit State			
		Damage		Collapse	
		λ [g]	β	λ [g]	β
Italy	5+-SS-B-MC	0.325	0.552	1.279	0.558
	5+-SS-B-SC	0.449	0.410	1.758	0.869
	5+-SS-B-W	0.291	0.543	1.695	0.540
	2/4-SS-B-MC	0.349	0.484	1.245	0.436
	2/4-SS-B-W	0.439	0.488	2.961	0.803
	RC-2/4-F-P	0.969	0.710	2.610	0.331
North Macedonia	RC-2-SS-B-W	0.783	0.354	4.406	0.524
	RC-3-SS-B-W	0.738	0.520	2.900	0.581
	RC-4-SS-B-W	0.691	0.523	2.740	0.591
	RC-3-F-P-W	0.906	0.619	3.201	0.876
Israel	RC-4/5-SS-B-MC	0.478	0.356	1.068	0.346
	RC-6+-SS-B-MC	0.283	0.262	1.343	0.075
	RC-4/5-C-BO-SC	0.251	0.568	1.343	0.075
	RC-2/3-C-B-MC	0.602	0.263	1.258	0.207
	RC-4/5-C-B-MC	0.210	0.513	1.343	0.075
	RC-6+-SS-B-SC	0.283	0.470	1.343	0.075
	RC-4/5-C-BO-W	0.259	0.538	1.175	0.568



9. Conclusions

Two different methodologies were applied for the calculation of taxonomy-based fragility curves to be used for the seismic risk evaluation of the residential building stock of a province in Northern Algeria and bridge inventories in Italy, North Macedonia and Israel in the context of the EU funded projects ITERATE and INFRA-NAT, respectively.

Given the larger scope, resources available and the technical challenges inherent to projects that evaluate the fragility of very diverse types of buildings at a national level, the methodology implemented in ITERATE used overall more simplified approaches for each of the steps in the fragility curve calculation process than the ones used for INFRA-NAT that only focused on the case of bridges, which are more straightforward from a structural analysis point-of-view.

In the earthquake record selection process, the ITERATE project used readily available tools [13] to choose a set of accelerograms which were compatible with the UHS of the case study region without regard for the characteristics of the structures to be analyzed. For the INFRA-NAT project, a very recent intensity measure and record selection technique was used [14] whose implementation showed to be challenging since no tools were available and a preliminary analysis of the inventory had to take place to determine a suitable period range for AvgSa calculations. While AvgSa [14] shows much promise for its application in the assessment of existing structures' portfolios, further studies and tools need to be made available to prove its efficacy and improve its usability.

In terms of analysis, for ITERATE, simple SDOF numerical models were defined and calibrated specifically for a total of nine building classes used to characterize the existing building typologies in Algeria. The GEM Foundation's Risk Modeller's Toolkit [9] was used to analyze the performance of 200 SDOF models when submitted to a set of 40 ground motion records that were scaled to 10 increasing intensity levels, leading to a total of 80,000 analyses per taxonomy branch. While the simplicity of the SDOF models allowed for the processing of the huge workload to be done efficiently, it also causes the analysis to neglect possible concentration of damage and partial collapses in the structures due to irregular geometric configurations. It is also difficult, within such an approach, to properly incorporate the cyclic and hysteretic behavior that should be expected for buildings that were categorized only on the basis of material and geometrical layout, particularly the height or number of stories.

On the other hand, for INFRA-NAT, a more sophisticated modelling and analysis framework [11] was used to create detailed 3D finite element models of bridges subjected to bi-directional earthquake records and process the results to obtain fragility curves for each structure modelled to be later combined in to a taxonomy-based fragility curve. A minimum of 30 synthetic bridges were analyzed under the application of 30 bi-directional ground motion records for each of the seven intensity measure levels (total of 210 records per set), leading to a minimum total of 6,300 analyses per taxonomy. While the number of analyses is greatly reduced, the workload was much more time consuming than for residential building stock in ITERATE. Nevertheless, the great detail obtained in the analysis allowed for proper verification of the results and lead to a much better understanding of the sources of vulnerability of the structures analyzed.

Overall, both methodologies were successful in their goal of obtaining fragility models for their implementation in large scale assessment of structure portfolios and further validation studies are on the way, to compare these fragility models with the more accurate ones, obtained from detailed MDOF numerical models of the existing buildings.

10. Acknowledgements

This work received financial support from both the ITERATE project (www.iterate-eu.org) "ECHO/SUB/2016/740181/PREV23 – ITERATE – Improved Tools for Disaster Risk Mitigation in Algeria" and the INFRA-NAT project (www.infra-nat.eu) co-funded by the European Commission DG-ECHO – Humanitarian Aid and Civil Protection. Project reference: 783298 – INFRA-NAT – UCPM-2017-PP-AG.



11. Copyrights

17WCEE-IAEE 2020 reserves the copyright for the published proceedings. Authors will have the right to use content of the published paper in part or in full for their own work. Authors who use previously published data and illustrations must acknowledge the source in the figure captions.

12. References

- [1] B. Zhao, F. Taucer, T. Rossetto (2009). Field investigation on the performance of building structures during the 12 May 2008 Wenchuan earthquake in China, *Engineering Structures*, 31, 1707-1723.
- [2] D. Perrone, P.M. Calvi, R. Nascimbene, E.C. Fischer, G. Magliulo (2018). Seismic performance of non-structural elements during the 2016 Central Italy Earthquake, *Bulletin of Earthquake Engineering*. <https://doi.org/10.1007/s10518-018-0361-5>
- [3] N. Achour, M. Miyajima, M. Kitaura, A. Price (2011). Earthquake-Induced Structural and Nonstructural Damage in Hospitals, *Earthquake Spectra*, 27, 617-634.
- [4] N. Ahmad, Q. Ali, H. Crowley, R. Pinho (2014). Earthquake loss estimation of residential buildings in Pakistan, *Natural Hazards*, 73, 1889-1955.
- [5] G. J. O'Reilly, D. Perrone, M. Fox, R. Monteiro, A. Filiatrault (2018). Seismic assessment and loss estimation of existing school buildings in Italy, *Engineering Structures*, 168, 142-162.
- [6] A. Di Meo, B. Borzi, M. Favarelli, M. Pagano, P. Ceresa, R. Monteiro (2018). Seismic vulnerability assessment of the urban building environment in Nablus, Palestine, *International Journal of Architectural Heritage*, 12, 1196-1215.
- [7] Villar-Vega, M., Silva, V., Crowley, H., Yepes, C., Tarquea, N., & Acevedo, A. (2017). Development of a Fragility Model for the Residential Building Stock in South America. *Earthquake Spectra*.
- [8] R. Salic, V. Sesov, K. Edip, E. Zuccolo, R. Monteiro, M. Vitanova, S. Micajkov, B. Petreski. (2019). Seismic Hazard and Earthquake Accelerogram Selection for Structural Analysis of Bridges in Republic of N. Macedonia. *18th International Symposium of Macedonian Association of Structural Engineers (MASE 2019)*. Ohrid, North Macedonia.
- [9] Silva, V., Casotto, C., Rao, A., Villar, M., Crowley, H. and Vamvatsikos, D. (2015). Open-Quake Risk Modeller's Toolkit - User Guide. *Global Earthquake Model*. Technical Report 2015-09.
- [10] ITERATE Project (2018). Deliverable DE2: Calibrated Numerical Models for Buildings of Typical Classes, *Brussels: European Civil Protection and Humanitarian Aid Operations*.
- [11] Borzi, B., Ceresa, P., Franchin, P., Noto, F., Calvi, G. M., & Pinto, P. E. (2015): Seismic Vulnerability of the Italian Roadway Bridge Stock. *Earthquake Spectra*, 31(4), 2137-2161.
- [12] McKenna, F. (2011): OpenSees: A Framework for Earthquake Engineering Simulation. *Computing in Science & Engineering*, 58 - 66.
- [13] Macedo, L., & Castro, J. (2017) SeEQ: An advanced ground motion record selection and scaling framework. *Advances in Engineering Software*, 114, 32-47.
- [14] Kohrangi M, Bazzurro P, Vamvatsikos D, Spillatura A. (2017): Conditional spectrum-based ground motion record selection using average spectral acceleration. *Earthquake Engng Struct. Dyn.* 46: 1667–1685.
- [15] Baker, J. W. (2015). Efficient Analytical Fragility Function Fitting Using Dynamic Structural Analysis. *Earthquake Spectra*, 31(1), 579-599.